VOLUME 10 ISSUE 1 2024

ISSN 2454 – 3055

INTERNATIONAL JOURNAL OF ZOOLOGICAL INVESTIGATIONS

Forum for Biological and Environmental Sciences

Published by Saran Publications, India

International Journal of Zoological Investigations Vol. 10, No. 1, 417-429 (2024)

International Journal of Zoological Investigations

Contents available at Journals Home Page: www.ijzi.net

Editor-in-Chief: Prof. Ajai Kumar Srivastav

Published by: Saran Publications, Gorakhpur, India

ISSN: 2454-3055

Studies on the Antimicrobial and Cytotoxic Effects of Silver Nanoparticles Synthesized from *Homonoia riparia* Lour Leaf Extract

Narayana Gupta C.H.L.D.S. and Subba Rao M.*

Department of Chemistry, Acharya Nagarjuna University, Nagarjuna Nagar 522510, Andhra Pradesh, India

**Corresponding Author*

Received: 6th November, 2023; **Accepted:** 26th December, 2023; **Published online:** 14th March, 2024

https://doi.org/10.33745/ijzi.2024.v10i01.046

Abstract: *Homonoia riparia* Lour *(H. riparia)* leaf extract was used in the current study to reduce silver nitrate's chemical reduction, resulting in green synthesis of silver nanoparticles to test the antibacterial activity and cytotoxic effects. The plant *H. riparia* was chosen due to the presence of reducing agents and the need for more information on the synthesis of silver nanoparticles using said plant. Environmentally friendly method was developed in this study for synthesising AgNPs from *Homonoia riparia* Lour *(H. riparia)* leaf extract. UV-vis absorption, XRD, and EDX analyses verified the synthesis of AgNPs. Analysis by SEM and TEM revealed that AgNPs were roughly spherical in shape and 27 nm in size. Maximum absorbance was measured between 440 and 450 nm, the zeta potential was -23.4 mV, and the powder crystal structures were cubic. The absorbance of AgNPs peaked between 400 and 430 nm. The MICs (mg/ml) of the synthesised AgNPs on *Staphylococcus aureus* ATCC 29213, *Escherichia coli* ATCC 10536, *Pseudomonas aeruginosa* ATCC 15442, and *Klebsiella pneumoniae* producing carbapenemase ATCC BAA-2146 were tested. After verifying the preliminary analysis results, which showed that all of the tested samples have cytotoxic potential, their cytotoxic activity was again evaluated, this time against the same strains, to determine the IC_{50}. Values were expressed as a percentage of cell growth inhibition at 50 ⍰M (sample 1), 100 ⍰M (sample 2), 150 ⍰M (sample 3) and 200 ⍰M concentrations (sample 4). AgNPs are still effective against pathogenic microorganisms when used at lower doses and exhibit a more potent antibacterial effect.

Keywords: Antimicrobial agent, Cytotoxicity, Silver nitrate, Surface Plasmons, Green synthesis, Reducing agents

Citation: Narayana Gupta C.H.L.D.S. and Subba Rao M.: Studies on the antimicrobial and cytotoxic effects of silver nanoparticles synthesized from *Homonoia riparia* Lour leaf extract. Intern. J. Zool. Invest. 10(1): 417-429, 2024.

https://doi.org/10.33745/ijzi.2024.v10i01.046

Introduction

The biological synthesis method (biosynthesis) is an environmentally friendly method involving plant extracts or microorganisms to reduce several types of metal ions. Living organisms can produce intracellular or extracellular nano-particles, where the latter is mainly implemented by researchers due to its low cost and because it is adaptable. The use of plant extracts, as in the current study, may be faster than the implementation of microorganisms for the

formation of silver nanoparticles. The use of living organisms in the synthesis of nanomaterials is consistent with the tenets of green chemistry. So-called "green synthesis" of metal nanoparticles involves using cheaper, less dangerous, more easily biodegradable, and more environmentally friendly materials (Singh *et al*., 2014). More and more nanotechnology studies are shifting their focus to the environmentally benign, correct, and cost-effective synthesis of metallic nanoparticles utilizing organic sources. This is because it eliminates the need to use toxic chemicals in the reduction processes (Uzair *et al*., 2020). Plants, bacteria, fungi, yeasts, and even viruses can all be used in the synthesis of metallic nanoparticles. When it comes to nanoparticle synthesis, plant-mediated green metal nanoparticle synthesis is highly regarded due to its neutral pH need and room-temperature occurrence. The synthesis reaction rate, the number of silver nanoparticles obtained, and their stability can be affected by variables such as the extract's nature and concentration, the concentration of the metallic salt, pH, and temperature (Zhang *et al*., 2020). Recent advances in the field of nanotechnology have had a strong impact in several areas, and the synthesis of silver nanoparticles has also followed this trend. The development of nanoscale silver particles has provided many exciting properties, ranging from electronic to biomedical applications (Bouafia *et al*., 2021). The main aspects of synthesising silver nanoparticles focus on the ability to control their size, shape and dispersion. In addition, silver nanoparticles are currently considered an important class of nanomaterials, being used mainly as catalysts or antibacterial and antifungal agents. The existence of a wide variety of metallic nanoparticles is related to their chemical nature (metals, metallic oxides, biomolecules, polymers), size and shape (spheres, cubes, tubes), state of dispersion (individually dispersed or agglomerated), dispersion medium and coating. After synthesis, the obtained nanoparticles must undergo characterization processes. Characterization is essential to control the synthesis conditions and organize the best ways of applying them. Reports on silver nanoparticles' antibacterial and cytotoxic potential can be observed in abundance in the current literature (Zhang *et al*., 2020; Saleh *et al*., 2023). However, despite their well-known efficiency, their mechanism of action still needs to be fully understood. This is quite complex and still has some differences. According to Ettaboina *et al*. (2022), silver nanoparticles have a great affinity with groups that have sulfur and phosphorus, which are elements found in the composition of cell membranes.

Herbal therapies are becoming accepted forms of primary care in many countries. They might be a source of unidentified antibacterial chemicals (Kaliyaperumal *et al*., 2013). Plants belonging to the Euphorbiaceae family were long thought to possess potential medicinal properties for treating various illnesses. *Homonoia riparia* Lour. has gained recognition for its medicinal properties (Xavier *et al*., 2015). The pulverized rhizome of this botanical specimen exhibits laxative, diuretic, and emetic properties. Despite the therapeutic benefits of *H. riparia*, there is limited knowledge regarding its antibacterial activity and phyto-constituents (Bapat *et al*., 2015). *H. riparia* is mostly recognized for its antioxidant and nephro-protective properties, as documented by Xavier *et al*. (2017). Silver nanoparticles (AgNPs) generated in plants have antibacterial qualities. However, no study compares these features to the plant's anticancer activity. Thus, given the botanical potential of *H. riparia* and considering the poorly explored biological and pharmacological possibility of the plant species of this biome, the current study aimed to assess the anti-microbial, anti-fungal, and anticancer properties of silver nanoparticles synthesized utilizing an ethanolic extract from the *H. riparia* leaf as a reducing agent.

Materials and Methods

Chemicals and Reagents:

All chemicals and reagents were of AR grade quality and 98-99% purity, all purchased from Sigma Aldrich, United States. All of the solutions

and reagents were made with double-distilled water (pH 7.02).

Plant material:

The leaves of *Homonoia Riparia* (Fig. 1) were collected in February 2018 from a reserve forest in the rural Guntur district (16.431555° N, 79.704394° E), Andhra Pradesh, India. Samples were compared to a specimen of the species housed in the Herbarium at Nagarjuna University's Department of Botany in Andhra Pradesh, India, to confirm its botanical identity. The obtained plant material weighed about 11.5 kg (leaves), and they were dried in an oven with fan-forced circulation at 45 °C for 7 days. After drying and complete stabilization of the material (removal of water and inactivation of enzymes), it was pulverized in a knife mill, obtaining dry powdered plant material with an approximate yield of 2 kg.

Fig. 1: *Homonoia riparia.*

Obtaining and fractioning the crude Homonoia riparia ethanolic extract (*HrEE*):

The dried and pulverized plant material was taken and then subjected to exhaustive maceration, using 95% ethanol as a solvent, in a stainless-steel container. Five extractions were performed, replacing the solvent every 72 h until the maximum depletion of the drug. After that, the extractive solution was solvent-distilled in a rotary evaporator at 50 °C and reduced pressure, finally obtaining the crude ethanolic extract (HrEE). The yield of HrEE was approximately 100 g of the total of this material (Lee *et al*., 2017).

Preliminary phytochemical screening:

The preliminary phytochemical analysis aimed to detect the main classes of secondary metabolites present in the crude ethanolic extract of *Homonoia riparia*. The techniques used for this purpose are based on chemical reactions that exhibit universal characteristics for each of the different classes of secondary metabolites investigated. The methodologies (Lee *et al*., 2017) used are carried out on a small scale, in test tubes, and the results are observed through sample reactions with specific reagent solutions for each metabolite class, which promote colour changes or precipitate formation.

AgNPs preparation:

The samples were prepared by following, with few modifications, the process described by Parthiban *et al*. (2019). The *H. riparia* ethanolic extract was made by boiling 10 g of leaf powder in 100 ml of double-distilled water for 10 min with a magnetic stirrer (model 752 A, 230V, Fisatom). The mixture was then centrifuged at a speed of 10,000 rpm for 15 min at 4 °C. The supernatant was collected, and then it was filtered using Whatman No. 1 filter paper. The ethanolic extract was maintained at 4°C before analysis. The silver nitrate ($AgNO_3$) that needed to be reduced was provided by Aldrich (USA). The best approach for producing silver nanoparticles was found to be dispersing the ethanolic extract of *H. riparia* in four concentrations of silver nitrate (5, 10, 25, and 50 mM) created using sterile double-distilled water. Four samples were produced by adding 1 ml of the ethanolic extract to containers containing 9 ml of each of the silver nitrate solutions. The mixtures were incubated for an hour at room temperature and without light. The solutions turned from pale yellow to deep brown, indicating the formation of silver nanoparticles.

Characterization of AgNPs:

The samples' absorbance was determined using an Elico-SL 210 model Double Beam UV-VIS Spectrophotometer. The Zeta Sizer Malvern

spectrophotometer and electrophoretic mobility assays were used to quantify particle size and zeta potential (Nano ZS90). JEOL JSM6490 Scanning Electron Microscope (SEM) was used to acquire the images. The device features a depth of focus of 0.5 mm and a backscattered electron detector. Energy dispersive spectroscopy (EDS) analysis was also performed with the same tools to identify the substances. A transmission electron microscope [LAB6 Transmission Electron Microscope with Model JEM-2100(HR)] was used to observe the morphology, dispersion and distribution of AgNP nanoparticles. PerkinElmer Spectrum One spectrometer was used to conduct Fourier-transform infrared spectroscopy (FTIR). The infrared spectra of silver nanoparticles (AgNPs) were acquired through the preparation of potassium bromide (KBr) pellets.

Antibacterial activity of H. riparia ethanolic extract:

The antimicrobial activity of the nanoparticle was evaluated through tests to determine the minimum inhibitory concentration (MIC) by the broth microdilution method as described by the Clinical and Laboratory Standards Institute (CLSI) (Patel, 2015). MIC is defined as the lowest concentration (mg/l) of an antimicrobial agent capable of inhibiting microbial growth. Inoculums were prepared with the growth of strains *S. aureus* ATCC 29213, *E. coli* ATCC 10536, *P. aeruginosa* ATCC 15442 and *K. pneumoniae* producing carbapenemase ATCC BAA-2146, incubated in Muller Hinton broth (MH). The concentration was adjusted by the turbidity of 0.5 on the Mcfarland scale, presenting approximately $1x10^8$ CFU (Colony Forming Unit)/ml, being adjusted between 0.08 - 0.10 of optical density with the aid of an optical density spectrophotometer at 625 nm. From the initial AgNP concentration, successive dilutions were performed with the aid of a multichannel pipette. Assays were carried out in ELISA microplates, flat-bottomed, in triplicate against each strain of bacteria. The plates are composed of 96 holes, identified by numbers (columns) and letters (rows) and each well in rows A, B, C, E, F and G had a final volume of 200 µl, receiving 80 µl of MH broth, 100 µl of AgNP solution and 20 µl of inoculum. Dilutions of cultures in MH broth resulted in a final concentration of $1x10^5$ CFU/ml per well. Controls received the following treatments:

- Growth control (H9, H10, H11 and H12): 180 µl of MH broth and 20 µl of inoculum;
- Pure broth (H1, H2, H3 and H4): 200 µl of Mueller Hinton broth;
- Broth + extract (line D): 100 µl of Mueller Hinton broth and 100 µl of AgNP (Performed so that the resulting staining of the plant extract with the MH broth was subtracted from the final absorbance result)

The plates were incubated in a bacteriological oven at 37°Cfor 24 h, and the procedure was performed in triplicate. The plates were read in a Multskan® microplate reader with a wavelength of 630 nm. The absorbance reading data obtained were calculated, indicating the percentage and inhibition achieved. Data repeatability analysis was performed by calculating the Intraclass correlation Interval at 95%, and IC_{50} calculations were performed by the methodology of fitting to the sigmoidal dose-response curve. Then, the lowest concentration value without microbial growth was accepted as the MIC value. The inhibition (or not) of the bacterial species was visually evaluated using the colourimetric reagent 2,3,5-triphenyl-tetrazolium chloride (CTT) at 2%. Then, the determination of the minimum bactericidal concentration (MBC) was performed by transferring a small aliquot (10 µl) of the contents of the wells where there was no visible bacterial growth in the MIC test to the surface of Petri dishes containing Müller-Hinton agar sterile. Samples of silver nanoparticles in aqueous medium were diluted serially from a starting concentration of 100% to determine their MIC and initial test of cytotoxic activity.

In vitro cytotoxicity tests:

In vitro cytotoxicity assays were performed, allowing investigation of the cell's vitality and

metabolic state. This colourimetric study converts 3- (4, 5-dimethyl-2-thiazole)- 2, 5 -diphenyl- 2-H-tetrazolium bromide (MTT) salt into formazan blue using mitochondrial enzymes present only in metabolically active cells. The strains used were provided by the National Cancer Institute (India) (Table 1). These were grown in RPMI medium supplemented with 10% foetal bovine serum and 1% antibiotics and kept in a 37°C oven with 5% CO_2. After being diluted in DMSO to obtain stock amounts of 20 mg/ml, samples (Table 1) were tested at a single concentration of 200 g/ml for all compounds.

Cells were plated at a density of $0.1X10^6$cells/ml for the SNB-19 and PC3 strains and $0.7X10^5$ cells/ml for the HCT-116 strains. In an oven, the plates were exposed to the chemicals for 72 h at 37 °C in a 5% CO_2 atmosphere. They were centrifuged at the end of this period, and the supernatant was removed. The plates were then incubated for 3 h in 150 L of MTT solution (tetrazolium salt). After the incubation period, the plates underwent another round of centrifugation to eliminate the MTT solution. The formazan precipitate was dissolved in 150 L of pure DMSO, and the absorbance at 595 nm was measured using a plate spectrophotometer. The mean standard deviation (SD) was used to calculate the % inhibition of cell growth in single-concentration testing. The cytotoxic potential of the tested samples was assessed using an intensity scale: no activity (NF), little activity, cell growth inhibition ranged from 1 to 50%, moderate activity, ranged from 50 to 75%, and a lot of activity, medium activity, ranged from 75 to 100%. To compute the IC_{50} (inhibitory concentration at 50%), the extracts that showed significant effects (above 75% inhibition) were again tested *in vitro* against the same cancer cell lines. Data processing and testing were carried out in parallel.

Results and Discussion

Preliminary pharmacognostic analysis to characterize *H. riparia* leaves yielded results of water content of 7.16 ± 0.51% and total ash content of 6.68 ± 1.12%. The analysis of the dry residue from the ethanolic extract used in the synthesis was performed in quadruplicate, showing a result of 1.04 ± 0.08% and the density was 0.9991 g/cm^3 at 20.01°C. After analysing the crude ethanolic extract of *H. riparia,* it was possible to suggest the presence of alkaloids, known for their antimicrobial, analgesic, anti-inflammatory, anti-fungal, antiviral, antioxidant action etc.; anthocyanins, which have antioxidant action; anthraquinones, with anticancer, anti-inflammatory, antimicrobial action; phenolic compounds, triterpenes and sterols, which have several important biological activities, with emphasis on antioxidant and cytotoxic activities; coumarins, with antimicrobial, anticancer, anti-oxidant action; lignans, with antitumor, anti-fungal, antioxidant, anti-inflammatory action, etc.; mono, sesqui and diterpenes, known to have anticancer, analgesic, anti-inflammatory, neuro-protective action; naphthoquinones, with antimicrobial, antiviral, antitumor; saponins, with emphasis on its anticancer action; and tannins, with antiulcerogenic action, antimicrobial, antiparasitic, antiviral, antioxidant, anti-inflammatory etc. (Debnath *et al*., 2018; Hamelian *et al*., 2018).

Synthesis of silver nanoparticles (*AgNPs*):

The ethanolic extract of *H. riparia* was used as a reducing agent in a single step of green production of silver nanoparticles at room temperature. It was feasible to visibly see a change in the hue of the solutions after 1 hour of incubation of the combinations in the absence of light and at room temperature. The colour changed from bright yellow to dark brown, indicating the creation of silver nanoparticles (Fig. 2). The colour shift is the first indication of the creation of silver nanoparticles, which is confirmed by UV-Visible spectroscopy.

SPR peak analysis by UV-Visible absorbance:

UV-Visible spectrophotometry scanning in the wavelength range of 200 to 800 nm was used to examine the biosynthetic processes of silver nanoparticles. The SPR peaks in this study were

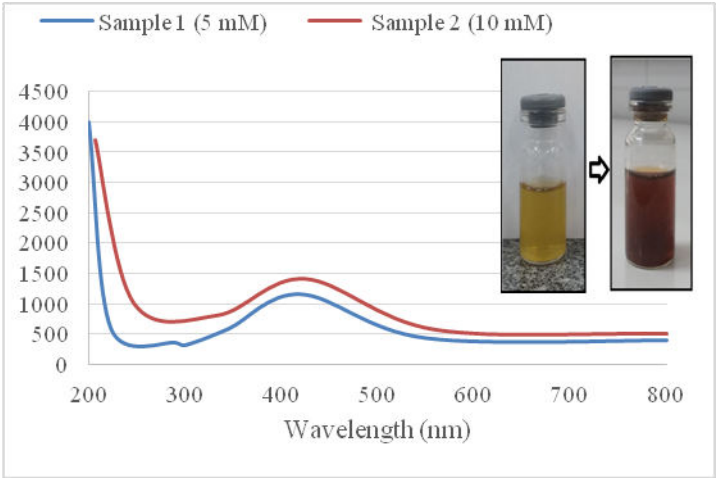

Fig. 2: Representative formation curves of UV-Vis absorbance measurements of silver nanoparticles obtained by green synthesis and (b) Silver nanoparticle biosynthesis reaction with colour change.

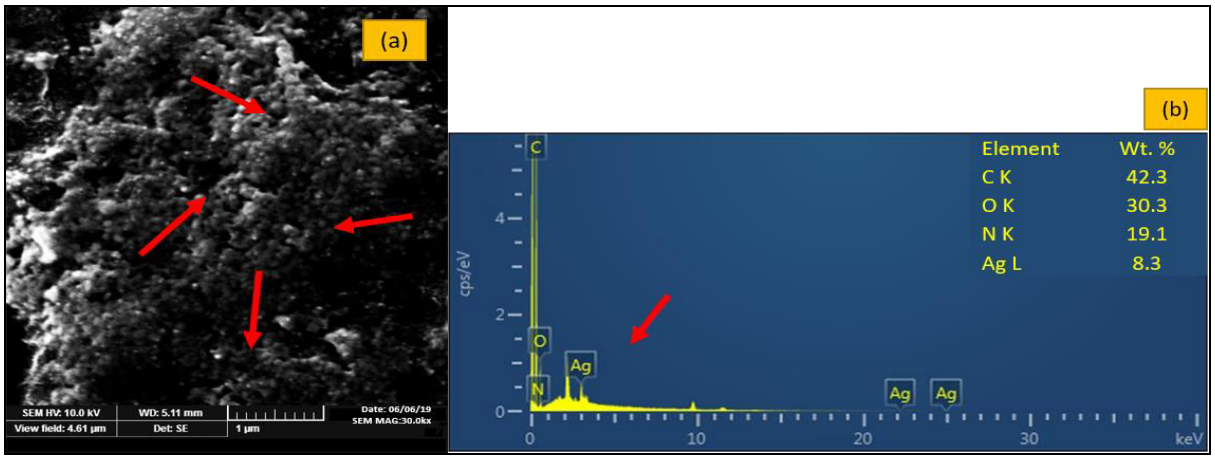

Fig. 3: (a) SEM images of silver nanoparticles obtained by green synthesis (b) EDX spectra for identification of chemical components present in samples of silver nanoparticles at 5 mM concentration.

between 420 and 424 nm. Figure 2 depicts the findings of the UV-Vis spectrophotometry analyses. It is feasible to see that the samples obtained had absorbance peaks below 430 nm, indicating that silver nanoparticles were synthesized (AgNPs). Because of their surface plasmonic resonance, AgNPs absorb electro-magnetic radiation at 420 to 500 nm wavelengths. The peak in the UV-Vis analysis (the SPR peak, i.e., surface plasmon resonance") results from surface electron oscillations in response to electro-magnetic radiation at a specific wavelength. This peak is associated with a distinctive colour variation that ranges from reddish brown to dark brown (Shiralgi *et al*., 2015).

SEM-EDX analysis:

Observing the shape and content of samples is part of the characterization stages for nano-materials research. SEM was used to examine the morphology of the silver nanoparticles obtained in this study. Analysing Figure 3, it is easy to see that the nanoparticles typically had a spherical morphology, moderate dispersion, and aggregation zones. The microscope morphological results are supported by UV-Vis research because Mie's theory predicts only a single plasmonic band in the absorption spectra of spherical nanoparticles, with SPR peaks ranging from 350 to 550 nm. In turn, energy-dispersive X-ray spectroscopy (EDS) is an analytical method for

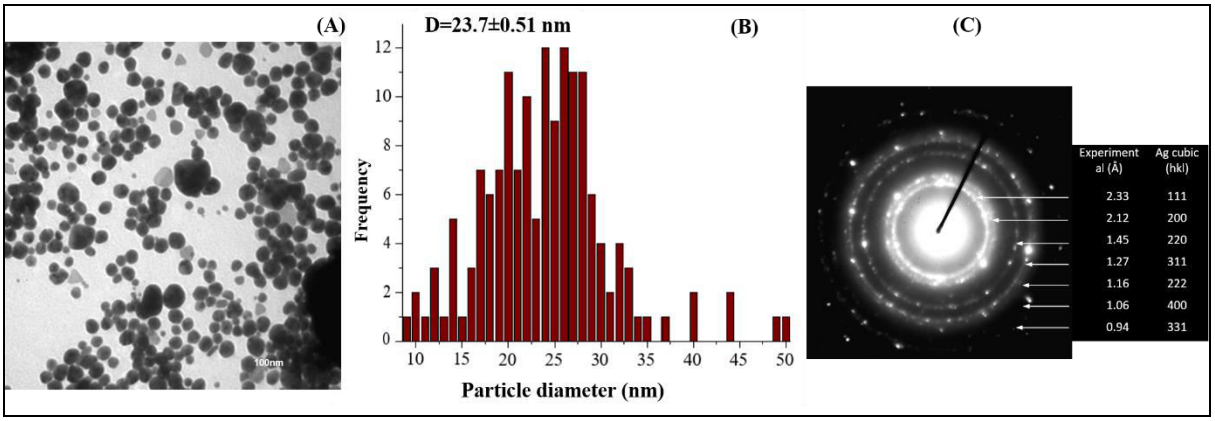

Fig. 4: TEM image of silver nanoparticles (A) TEM image (B) Histomgram (C) Electron Diffraction Pattern of Silver Nanoparticles.

elemental determination critical to characterisation. It is typically used with scanning or transmission electron microscopy analysis to offer information on the chemical element distribution in silver nanoparticles (AgNPs). Furthermore, it is a precious method for detecting the presence of these nanoparticles in complex materials (Tahir *et al*., 2015). Energy dispersive spectroscopy analyses revealed typical signals in the silver area in the current study, demonstrating the creation of silver nanoparticles. Figure 4 depicts the obtained spectra (A-D). Due to the surface plasmon resonance phenomenon, metallic silver nanoparticles typically exhibit a peak of optical absorption at around 3 keV (Tahir *et al*., 2015).

TEM Analysis:

Figure 4 displays the TEM image (A) and matching histograms (B) of the silver nanoparticles produced in this manner. The largest nanoparticles generated in this experiment were achieved at a temperature of 85 °C and had an average diameter of 27 nm. It was possible to confirm the crystalline nature of the silver nanoparticles using the electron diffraction pattern (Fig. 4C). The face-centred cubic (fcc) structure of metallic silver can be used to index the interplanar distances of the diffraction rings (Luis López-Miranda *et al*., 2016).

Infrared Spectroscopy (*FTIR*):

FTIR is particularly beneficial for characterising metallic nanoparticles for identifying chemical species that interact with the particle surface. Polar groups like O-H, C=O, C=C, and N-H are particularly well-suited to this approach. For this investigation, the FTIR spectra of the generated nanoparticles as well as the $AgNO_3$ and leaf extract used as precursors were obtained (Fig. 5). In the spectrum, amide A (N-H bond tension vibrations) was allocated to the region at 3417 cm^{-1}, amide I (C=O bond tension vibrations) to the region at 1648 cm^{-1}, amide II (N-H bond flexural vibrations and C-N bond tension) to the region at 1535 cm^{-1}, and amide III to the region at 1240 cm^{-1} (flexural vibrations of the N-H bond). According to Sharma *et al*. (2019), the band corresponding to amide I the peak that provides the most useful information for examining the secondary structure of proteins like leaf extract. In the $AgNO_3$ spectra, the Ag^+ NO_3^- ion pair exhibits a prominent absorption band at 1376 cm^{-1}. Nonetheless, slight alterations in the absorption mentioned above zones can be seen when analysing the spectra of silver nanoparticles. As the NO_3^- ion is separated from its Ag^+ counterpart, the anion's electronic environment changes, shifting the free NO_3^- ion's distinctive peak at 1385 cm^{-1}. These results indicate that the amide groups in the leaf extract are reacting with the silver nanoparticles. The stability of colloidal solutions is greatly enhanced by these interactions.

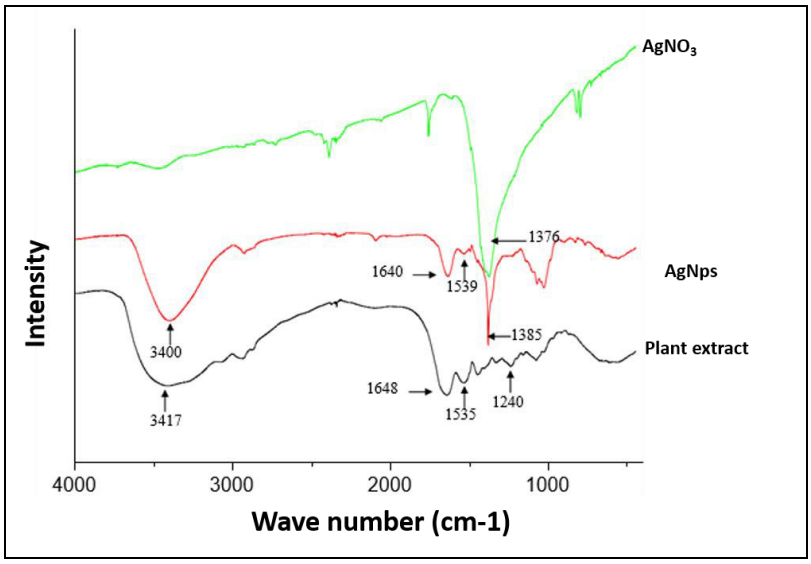

Fig. 5: FTIR spectra of the precursors used ($AgNO_3$ and Extract) and of the silver nanoparticles.

Antibacterial and cytotoxic activity of silver nanoparticles (*AgNPs*) *produced through green synthesis*:

A study carried out with silver nanoparticles obtained from extracts of *H. riparia* leaves evaluated their antimicrobial activity against *P. aeruginosa, K. pneumoniae*, *S. aureus* and *E-coli* by the standard method of diffusion in wells, finding significant effects against these bacteria. However, this assay only allows a qualitative analysis of the antimicrobial activity of AgNPs, and it is not possible to calculate their MIC (Riaz *et al*., 2022). The antibacterial effect of AgNP produced by green synthesis with *H. riparia* leaves and its pure ethanolic extract was evaluated by microdilution against *S. aureus* (gram-positive), *E. coli* and *P. aeruginosa* (gram-negative). These bacterial species are of great importance for the health system and have been used by other researchers to evaluate the antibacterial action of AgNPs obtained through green synthesis (Ozturk Fatma *et al*., 2019). The antimicrobial activity results obtained for AgNPs with HrEE are shown in Table 2.

AgNP made with HrEE showed antimicrobial action against both types of bacteria: gram-positive and gram-negative. *H. riparia* leaves have several constituents, such as gallic acid, tannins, flavonoids, unsaturated fatty acids and coumarin derivatives. It is then observed that the main constituents found are phenolic compounds, to which the antioxidant, antimicrobial and anticancer activities of the extract of *H. riparia* leaves are attributed. The FTIR spectrum (Fig. 5) and the measured zeta potential both show that chemical components from the *H. riparia* leaf extract were maintained in the nanoparticle. This property resulted in cell damage and subsequent bacterial death, increasing the bactericidal effectiveness against the two kinds of bacteria studied (Srećković *et al*., 2023). Based on the action of a specific antagonist against adhesion proteins on the bacterial surface, it has already been shown to have an inhibitory effect on infections brought on by gram-positive bacteria of the *S. aureus* type. This action prevents adhesion to epithelial cells (anti-adherent effect) and the subsequent penetration of the bacteria. Condensed tannins, which are found in the extract, would be responsible for this antibacterial activity (Srećković *et al*., 2023).

According to studies, coumarins, tannins, and phenolic chemicals are mostly to blame for this plant's reducing characteristic, which improves its reducing capacity required for the synthesis of AgNPs and may be what gives it the anticipated

Table 1: *In vitro* cytotoxic activity of AgNPs against tumour cell lines

Sample		SNB-19	SD (±)	PC3	SD(±)	HCT-116	SD(±)
Sample no.- (Conc.)	**Identification**	**Inhibition% (average)**		**Inhibition% (average)**		**Inhibition% (average)**	
1- (5 mM)	50%	94.92	0.35	97.99	0.49	99.09	0.68
	25%	84.17	0.37	94.25	1.47	94.84	0.85
	12.50%	79.8	0	63.35	3.43	92.4	0.23
	6.25%	25.46	5.58	38.12	9.31	34.09	0
2- (10 mM)	50%	96.16	0.3	98.55	0.49	99.83	0.17
	25%	96.54	0.52	92.06	0.56	96.09	0.17
	12.50%	91.27	3.87	95.01	4.51	98.81	0.17
	6.25%	56.23	0	70	0.69	91.83	0.79
3- (25 mM)	50%	99.16	0.15	99.93	0.29	100	0.06
	25%	95.16	0.6	98.96	0.1	100	1.08
	12.50%	90.37	1.26	96.81	1.37	98.13	0.11
	6.25%	81.74	1.12	94.46	0.59	97.66	0.34
4- (50 mM)	50%	98.32	0.45	99.52	0.1	100	0.06
	25%	97.17	0.2	99.65	0.1	100	0.07
	12.50%	97.05	0.15	99.45	0	100	0.06
	6.25%	82.01	2.23	93.49	3.53	98.58	0.17

Values expressed as a percentage of cell growth inhibition ± standard deviation (SD).

Table 2: MIC of obtained with AgNPs through the broth microdilution method (mg/ml)

Statistics (mg/ml)	*S. aureus* (Gram-positive)		*E. coli* (Gram-negative)		*P. aeruginosa* (Gram-negative)		Carbapenemase-producing *K. pneumoniae*	
	HrEE	AgNPs	HrEE	AgNPs	HrEE	AgNPs	HrEE	AgNPs
MIC (IC_{50})	84.98	12.04	267.01	71.37	10000	17.06	21.11	0.85
IC (IC_{50})	67.25	5.88	192.3	69.03	very wide	16.24	12.57	0.01
	107.4	24.65	372.6	98.87		23.75	35.39	7.23
$IC_{99.9}$(MBC)	8413.02	1192	26433	7065.6	990000	1688.94	2088.9	84.15

antibacterial action (Srećković *et al*., 2023). AgNPs also have a high surface area that is open to contact, so it is predicted that the smaller they are, the greater the rise in their bactericidal impact, interacting not only with the membrane's surface but also entering inside the bacterium (Rajkuberan *et al*., 2017). As can be seen in the 96-well plates in Figure 6, it was chosen to test them against a multidrug-resistant bacterium, the carbapenemase-producing *K. pneumoniae*, in light of the findings obtained against gram-negative bacteria.

Cytotoxic activity of AgNPs:

The use of silver nanoparticles as a safe and efficient method in the treatment of cancer is still a complex task. However, studies that aim to understand the antitumor efficiency of silver are progressing intensely. The reproducibility and stability of these silver nanostructures are key objectives for researchers dedicated to the development of this area, the so-called "nanomedicine". There is strong evidence that silver nanoparticles insert themselves into target cells and reprogram them, triggering mainly the phenomenon of apoptosis (Cheng *et al*., 2021). The green synthesis of silver nanoparticles appears as

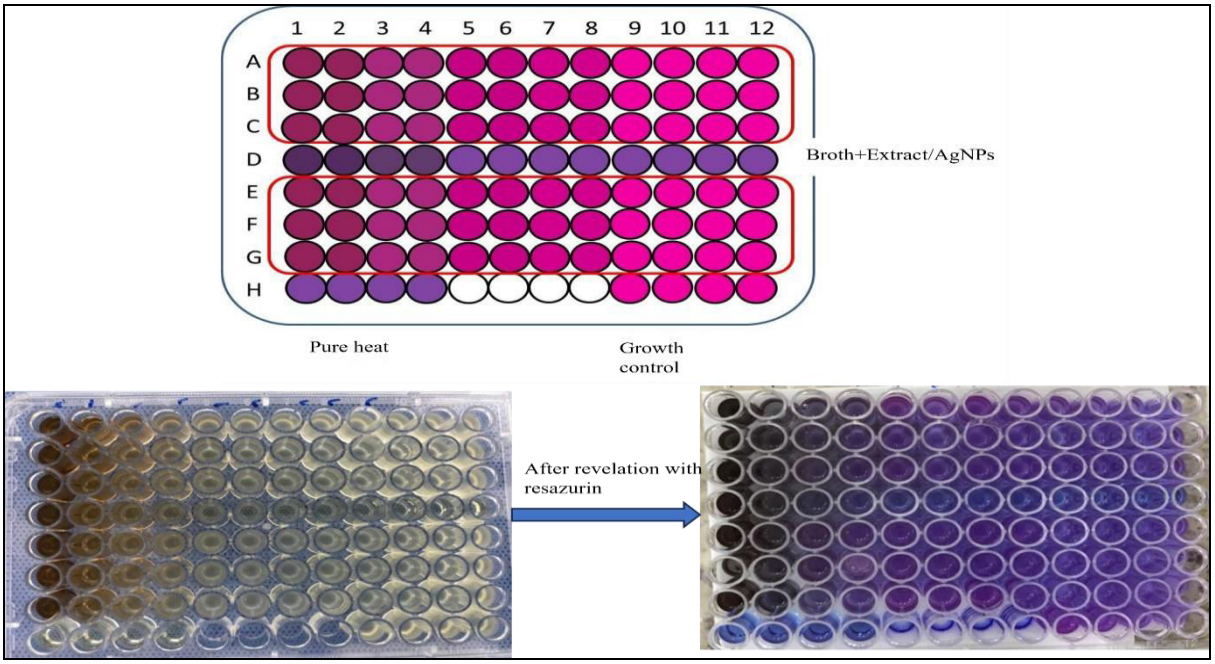

Fig. 6: Microdilution test plates before and after resazurin development: AgNP x carbapenemase-producing *K. pneumoniae.*

an interesting alternative for this purpose since the silver reducing agent, which is usually some chemical substance, is replaced by biomolecules from the living organism used (plant), thus reducing the use of toxic and expensive chemicals. Among the many advantages of green synthesis are its cost-effectiveness, good reproducibility and lower amount of energy needed compared to other methods (Marischa Elveny *et al*., 2021).

In the present work, a preliminary study (screening) was initially carried out to evaluate the cytotoxic capacity of silver nanoparticles obtained by green synthesis against three tumour cell lines. Concentrations obtained by serial dilutions from 100% of the solution initially obtained were used in the test, totalling four concentrations: 50%, 25%, 12.5% and 6.25%. The results obtained with the screening of the tested samples are shown in Table 1.

The data in Table 1 demonstrate that all tested substances were effective and exhibited highly significant cytotoxic activity, above 75% of inhibition, with emphasis on the HCT-116 strain (colon cancer), where all samples showed an inhibition rate above 90%. With regard to the SNB-19 strain (astrocytoma), samples 3 and 4 showed the best results, with an inhibition rate between 82 and 99%, whereas, against this same strain, samples 1 and 2 showed activities from low to moderate, with inhibition rates between 25.46% (6.25% AgNPs dilution for sample 1) and 56.23% (6.25% AgNPs dilution for sample 2).

Regarding the PC3 strain (prostate cancer), only sample 1 (6.25% dilution of AgNPs) showed a cytotoxic activity considered low (inhibition rate of 38.12%), whereas all other samples showed a good inhibition rate (above 75%), with emphasis on sample 4, where all the concentrations used demonstrated an inhibition rate above 90%.

After verifying the results obtained in the preliminary analysis, where it was possible to conclude that all the tested samples have cytotoxic potential, they had their cytotoxic activity evaluated again against the same strains, this time to determine the IC_{50}, which is the necessary concentration for that half the maximum effect is

Table 3: *In vitro* cytotoxic activity (IC_{50}) of silver nanoparticles obtained by green synthesis against tumour cell lines

Cell line (Lineage)	IC_{50} µM (range)*				
	Sample 1 (50 µM)	Sample 2 (100 µM)	Sample3 (150 µM)	Sample 4 (200 µM)	Doxorubicin**
SNB-19	7.76	8.66	10.18	8.07	1.2
	5.62 – 10.72	7.97 – 9.42	8.08 – 12.82	5.78 – 11.26	1.03-1.39
PC3	11.37	14.16	6.43	2.93	0.44
	4.51 – 28.71	8.20 – 24.48	4.87 – 8.49	2.14 – 4.01	0.34-0.54
HCT-116	21.55	26.88	5.41	4.35	0.11
	20.62 – 22.52	23.26 – 31.05	4.67 – 6.27	4.23 – 4.47	0.08-0.14

Mean inhibitory concentration (IC_{50}) values with a 95% confidence interval were obtained by nonlinear regression from two independent experiments. **Doxorubicin was used as a positive control. Values expressed as percentage of cell growth inhibition ± standard deviation

achieved (50% inhibition rate). Values were expressed as percentage of cell growth inhibition at concentrations of 50 µM (sample 1), 100 µM (sample 2), 150 µM (sample 3) and 200 µM (sample 4). Detailed IC_{50} data of the tested samples are shown in Table 3.

The data in Table 3 shows that the samples presented cytotoxic potential ranging from moderate to high for the tested tumour cell lines. Samples 1 and 2 showed better activity for the astrocytoma cell line (SNB-19) with IC_{50} of 7.76 and 8.66 µM, respectively. Sample 3 was more cytotoxic for the colon cancer cell line (HCT-116 - 5.41 µM). The best activity was observed in sample 4, where the IC_{50} rate was only 2.93 µM for the prostate cancer cell line (PC-3). There are several reports in the literature about the cytotoxic potential of silver nanoparticles obtained by green synthesis, however, in the genus *Jatropha*, there is no study, and this is also the first work carried out with the genus and with the species *H. riparia*.

For the analysis of the antimicrobial activity of silver nanoparticles, strains of *K. pneumoniae* that produce ATCC BAA-2146 carbapenemase were used, carrying the bla_{KPC} gene that confers resistance to carbapenem antibiotics (Ertapenem, Meropenem and Imipenem). The results obtained were the following: The result of the minimum inhibitory concentration (MIC) of the antibacterial activity of AgNPs was 0.85 mg/ml (Table 2), which, according to Aligiannis *et al*. (2001) frame it as a moderate inhibitor for carbapenemase-producing *K.pneumoniae*. Given the known complexity of its treatment, this result represents an up-and-coming alternative in the fight against infections caused by the microorganism mentioned above.

There are several reports in the literature about the antibacterial potential of silver nanoparticles obtained by green synthesis; however, in *H. riparia*, there are few studies, ours being the first work carried out with the species *H. riparia*. Chauhan *et al*. (2016) carried out a study with the species *J. curcas*, using the ethanolic extract of the leaves for the biosynthesis of silver nanoparticles (AgNPs) and subsequent evaluation of their antibacterial potential against food pathogens.

It is important to emphasize that the demand for new drugs with action against multidrug-resistant bacteria is a worldwide need since, in 2017, the WHO published a list containing the "priority pathogenic agents" in an attempt to guide and promote research and development of new antibiotics in line with current public health priorities. This list comprises 12 families of bacteria divided into 3 categories: critical, high or medium priority, with the Enterobacteriaceae family, resistant to carbapenem and *Klebsiella*,

being in the highest priority group, that of multiresistant bacteria.

UV-Vis analysis of the nanoparticles indicated that the SPR peak occurred at 450 nm. Study by TEM showed that the AgNPs biosynthesized by these seven extracts,mainly were spherical and the zeta potential (from -26 to -35) indicated a high colloidal stability. With regard to cytotoxic activity, this study observed that samples of biosynthesized AgNPs showed promising results against human lung cancer cells, attributing this activity to the chemical constitution of the plant extracts used (Hamelian *et al*., 2018).

Rajkuberan *et al*. (2017) carried out a study with the species *Euphorbia antiquorum* L. (Euphorbiaceae), using the aqueous extract of its latex for the biosynthesis of silver nanoparticles (AgNPs) and subsequent evaluation of its cytotoxic potential. This experimental data corroborates our work, as phytochemical studies carried out with *H. riparia* indicated the strong presence of phenolic compounds in its chemical constitution.

Conclusion

AgNPs have been shown to have potent antibacterial activity against pathogenic micro-organisms associated with foodborne illness at low doses. AgNPs are widely used in food packaging, which has the potential to improve food safety while also reducing food waste. However, further research into the migration of silver ions to food is required, and migration thresholds in terms of consumer health must be established. In contrast to traditional materials, antibacterial, low-cost, easily synthesised materials are becoming increasingly popular for use in food packaging. This study used an easy, cheap, and environmentally friendly method for producing AgNPs from *H. riparia* leaves. XRD, EDX, and UV-vis absorption analyses were used to validate the production of AgNPs. According to SEM and TEM examinations, AgNPs were spherical in shape and had an average size of about 27 nm. The particles were discovered to have a maximum absorbance between 440 and 450 nm, a zeta potential of -23.4 mV, and cubic powder crystal structures. The evaluation of their biological activities showed that these nanoparticles have significant antibacterial and cytotoxic potential, with high inhibition rates for all tested samples. The significant results obtained are probably due to the presence of phenolic compounds in the chemical constitution of the plant. These results are novel for the species, which supports additional research on this plant to clarify potential methods of action. Given the aforementioned, *H. riparia* had a wealthy chemical constitution from both a chemical and biological point of view, with the existence of biologically fascinating chemicals suggesting that this species has a lot of untapped potential. AgNPs have been found to have more decisive antibacterial action than antibiotics against foodborne pathogenic microorganisms, and they are still effective at lower doses. It is hoped that the widespread use of AgNPs in food packaging will improve food safety and waste. However, further research into the migration of silver ions to food is required, and migration thresholds in terms of consumer health must be established.

References

Aligiannis N, Kalpotzakis E, Mitaku S and Chinou IB. (2001) Composition and antimicrobial activity of the essential oils of two *Origanum* Species. J Agricult Food Chem. 49: 4168-4170.

Bapat UC and Mhapsekar DR. (2015) Evaluation of antioxidant activity of *Homonoia riparia* Lour., *Kirganelia reticulata* (Poir) baill., *Phyllanthus fraternus* Webster and *Pedilanthus tithymaloides* (Linn.) Poit. and its correlation with the total phenolic and flavonoid contents. Int J Pharma Bio Sci. 6:723-732.

Bouafia A, Laouini SE, Ahmed ASA, Soldatov AV, Algarni H, Feng Chong K and Ali GAM. (2021) The recent progress on silver nanoparticles: synthesis and electronic applications. Nanomaterials 11(9): 2318.

Chauhan N, Tyagi AK, Kumar P and Malim A. (2016) Antibacterial potential of *Jatropha curcas* synthesized silver nanoparticles against food-borne pathogens. Frontiers Microbiol. 7: 1-13.

Cheng Z, Li M, Dey R. and Chen Y. (2021) Nanomaterials for cancer therapy: current progress and perspectives. J Hematol Oncol. 14: 85.

Debnath B, Singh WS, Das M, Goswami S, Singh MK, Maiti D and Manna K. (2018) Role of plant alkaloids on human health: A review of biological activities. Materials Today Chem. 9: 56-72.

Ettaboina S, Nakkala K and Chathalingath N. (2022) Synthesis of silver nanoparticles and its application. Materials Characterization 1(2): 77-84.

Hamelian M, Hemmati S, Varmira K and Veisi H. (2018) Green synthesis, antibacterial, antioxidant and cytotoxic effect of gold nanoparticles using *Pistacia atlantica* extract. J Taiwan Institute Chem Engineers 93: 21-30.

Kaliyaperumal K, Jegajeevanram K, Vijayalakshmi J and Beyene E. (2013) Traditional medicinal plants: A source of phytotherapeutic modality in resource-constrained health care settings. Evidence-based Complem Alternat Med. 18: 67-74.

Lee IS, Jung Seung H, Kim CS and Kim J. (2017) Phenolic compounds from the leaves of *Homonoia riparia* and their inhibitory effects on advanced glycation end product formation. Natural Prod Sci. 23: 274.

Luis López-Miranda J, Borjas-Garcia SE, Esparza R and Rosas G. (2016) Synthesis and catalytic evaluation of silver nanoparticles synthesized with *Aloysia triphylla* leaf extract. J Clust Sci. 27:1989-1999.

Marischa Elveny, Afrasyab K, Ali Taghvaie N and Ahmad BA. (2021) A state-of-the-art review on the application of various pharmaceutical nanoparticles as a promising technology in cancer treatment, Arabian J Chem. 14(10): 103352.

Ozturk Fatma, Çoşkunçay S and Duman F. (2019) Biosynthesis of silver nanoparticles using leaf extract of *Aesculus hippocastanum* (horse chestnut): Evaluation of their antibacterial, antioxidant and drug release system activities. Materials Sci Engineering C. 107: 110207.

Patel JB, Cockerill RF, Bradford AP, Eliopoulos MG, Hindler AJ, Turnidge JD. WPMZLB. (2015). Methods for dilution antimicrobial susceptibility tests for bacteria that grow aerobically; Approved Standard. https://doi.org/10.1007/s00259-009-1334-3.

Phartiban E, Manivannan N, Ramanibai R and Mathivanan N. (2019) Green synthesis of silver nanoparticles from *Annona reticulata* leaves aqueous extract and its mosquito larvicidal and anti-microbial activity on human pathogens. Biotechnol Rep. 21: 1-9.

Rajkuberan C, Prabukumar S, Sathishkumar G, Wilson A, Ravindran K and Sivaramakrishnan S. (2017) Facile synthesis of silver nanoparticles using *Euphorbia antiquorum* L. latex extract and evaluation of their biomedical perspectives as anticancer agents. J Saudi Chem Soc. 21(8):911-919.

Riaz M, Suleman A, Ahmad P, Khandaker MU, Alqahtani A, Bradley DA and Khan MQ. (2022) Biogenic synthesis of AgNPs using aqueous bark extract of *Aesculus indica* for antioxidant and antimicrobial applications. Crystals 12(2): 252.

Saleh BH, Al-ugaili DN, Oraibi AG and Ibrahim RA. (2023) Antibacterial and cytotoxic activity of *Mentha arvensis* L. leaves methanolic extract *in vitro*. J Pure Appl Microbiol. 17(2):1221-1230.

Sharma K, Guleria S and Razdan V. (2019) Green synthesis of silver nanoparticles using *Ocimum gratissimum* leaf extract: characterization, antimicrobial activity and toxicity analysis. J Plant Biochem Biotechnol. 29(2): 213-224.

Shiralgi Y, Manjanna J, Peethamba S, Achur R and Satyanarayan N. (2013) Green synthesis of silver nanoparticles using *Acacia farnesiana* (Sweet Acacia) seed extract under microwave irradiation and their biological assessment. J Cluster Sci. 24:1081-1092.

Singh Priti and Jain S. (2014) Biosynthesis of nanomaterials: Growth and properties. Rev Adv Sci Engineer. 3(8): 231-238.

Srećković NZ, Nedić ZP, Monti DM, D'Elia L, Dimitrijević SB, Mihailović NR, Katanić Stanković JS and Mihailović VB. (2023) Biosynthesis of silver nanoparticles using *Salvia pratensis* L. aerial part and root extracts: Bioactivity, biocompatibility, and catalytic potential. Molecules 28(3): 1387.

Tahir K, Nazir S, Li B, Khan AU, Khan ZUH, Ahmad AK and Qudrat ZY. (2015) Enhanced visible light photocatalytic inactivation of *E. coli* using silver nanoparticles as photocatalyst. J Photochem Photobiol B Biol. 153: 261-266.

Uzair B, Liaqat A, Iqbal H, Menaa B, Razzaq A, Thiripuranathar G, Fatima Rana N and Menaa F. (2020) Green and cost-effective synthesis of metallic nanoparticles by algae: Safe methods for translational medicine. Bioengineering 7(4): 129.

Xavier S, Devkar R, Chaudhary S, Shreedhara C and Manganahalli M. (2015) Pharmacognostical standardisation and HPTLC quantification of gallic acid in *Homonoia riparia* Lour. Pharmacogn J. 7: 383-388.

Xavier S, Haneefa S, Devkar R, Picheswara M, Rajalekshmi S and Chandrashekara MM. (2017) Antioxidant and nephroprotective activities of the extract and fractions of *Homonoia riparia* Lour. Pharmacogn Mag. 13: 25-30.

Zhang D, Ma Xl, Gu Y, Huang H and Zhang G. (2020) Green synthesis of metallic nanoparticles and their potential applications to treat cancer. Front Chem. 799(8): 1-18.